Journal of Drug Delivery Science and Technology 64 (2021) 102627

Contents lists available at ScienceDirect

Journal of Drug Delivery Science and Technology

journal homepage: www.elsevier.com/locate/jddst

Sustained release of Ganoderma lucidum antitumor drugs using a sandwich structured material prepared by electrospinning

Jiahui Lu [a], Yanying Li [a], Anqiang Zhang [a,*], Weiming Liu [b], Xingli Wang [b], Fuming Zhang [c], Robert J. Linhardt [c,d], Zhibin Lin [e], Peilong Sun [a,**]

[a] College of Food Science and Engineering, Zhejiang University of Technology, 310014, Hangzhou, PR China
[b] Hangzhou Baishanzu Biotech Co. Ltd., 310052, Hangzhou, PR China
[c] Department of Chemical and Biological Engineering, Center for Biotechnology and Interdisciplinary Studies, Rensselaer Polytechnic Institute, 12180, Troy, NY, USA
[d] Departments of Chemistry and Chemical Biology and Biomedical Engineering, Biological Science, Center for Biotechnology and Interdisciplinary Studies, Rensselaer Polytechnic Institute, 12180, Troy, NY, USA
[e] State Key Laboratory of Natural and Biomimetic Drugs, Department of Pharmacology, School of Basic Medical Sciences, Peking University, 100191, Beijing, PR China

ARTICLE INFO

Keywords:
Sustained release
Ganoderma lucidum
Multi-compounded drugs

ABSTRACT

In cancer therapy, there still remains great challenges such as controlling cancer metastasis and the side effects from chemotherapy. Many anti-cancer drugs have cytotoxicity to normal cell with a high concentration, on the other hand, the anti-cancer effect will not be ideal if it didn't reach the effective concentrations. So there is a way to make balance between the cytotoxicity and effective concentrations, sustained release can not only prolong the duration of the effective concentration but also reduce the time of peak concentration. Herein, we designed a sandwich structured antitumor composite with a three-layer film including: i) the top and bottom layers of ethyl cellulose (EC) containing *Ganoderma lucidum* triterpenes (GLT); ii) the middle layer of polyvinyl alcohol (PVA) containing *G. lucidum* polysaccharides (GLP). The films were fabricated layer-by-layer using electrospinning with the aim of providing the sustained release of the antitumor activity of GLT and GLP for use in cancer therapy. This sandwich structured material has potential for sustained antitumor release, high loading capacity (1.6% for GLT and 7.9% for GLP) and large surface area. The morphology, structure, biocompatibility, and the release profile of the encapsulated GLP and GLT in this fabricated composite were characterized. The *in vitro* antitumor effects of this drug film were studied using carcinoma cells, as SGC-7901, A549, Hela and Caco-2, with the IC_{50} of 51.2, 90.7, 93.0 and 21.7 μg/mL, respectively. In brief, this medical film achieved a good antitumor effect at the cellular level.

1. Introduction

Sustained drug release has been widely studied around the world. Varieties of carriers have been applied for drug release, including microcapsules, liposome micro-particles and nanoparticles [1,2]. Electrospining fiber has unique advantages such as high specific surface area to volume ratio, nontoxic polymers for good biocompatibility and physiochemical properties, rapid drug dissolution and promoting tissue absorption, tunable release [3,4]. These materials usually can be easily modified to enhance the ratio of cells taking a drug, to capture cancer cells from the blood and to trap these in special 3D fibrous networkers [5]. The anticancer effects of materials with sustained release properties have been investigated for melanoma, human prostate cancer, hepatocellular carcinoma, breast cancer, cervical cancer and colorectal carcinoma [6]. The sustained release of antitumor drugs can not only be toxic to tumor cells, but also can restrict the proliferation and metastasis of these cells [7].

The anticancer activity of "Lingzhi" (*Ganoderma lucidum*, a popular medicinal mushroom) has been investigated in both *in vitro* and *in vivo* studies, supporting its application for cancer treatment and prevention [8]. *G. lucidum* polysaccharides (GLP) and triterpenes (GLT) are the main bioactive components with anticancer activity [9,10]. Recently, researchers reported that GLP could be embedded in biocompatible polymers for sustained release [11,12], but reports about the sustained

* Corresponding author.
** Corresponding author.
E-mail addresses: 417434934@qq.com (J. Lu), zhanganqiang@zjut.edu.cn (A. Zhang), sun_pl@zjut.edu.cn (P. Sun).

https://doi.org/10.1016/j.jddst.2021.102627
Received 25 March 2021; Received in revised form 19 May 2021; Accepted 23 May 2021
Available online 29 May 2021

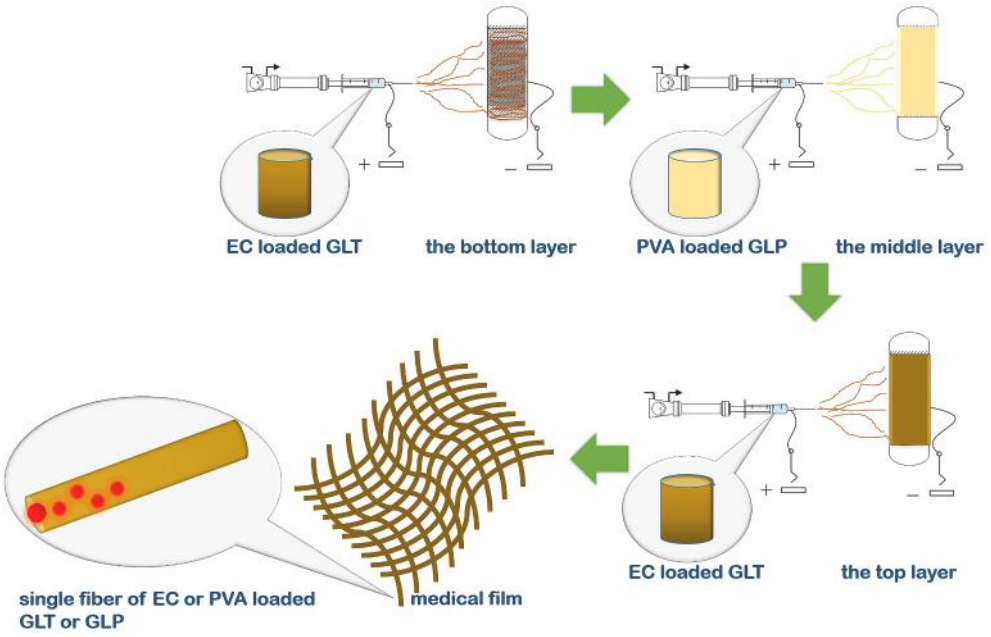

Scheme 1. The fabrication of sandwich structure films.

release of GLT were fewer. GLT was found to have slight cytotoxicity to normal cells with a high concentration [13,14], if we can control its release rate, the side effect will be reduced.

Recently, electrospinning techniques have become an important strategy for use in drug delivery systems [15]. The electrospun fibers with high surface-to-volume ratios can improve processes including cell binding and proliferation, drug loading, and mass transfer processes [16]. Numerous electrospun materials have been used for controlled release of bioactive substances including antibiotics, anticancer agents and macromolecules, such as proteins and DNA. The major advantage of the electrospinning method is that a wide variety of low solubility drugs can be loaded into the fibers to improve their diffusion rate, bioavailability and be controlled release [17]. In addition, these drug delivery fibers can maximizes encapsulation efficiency and drug loading capacity for combined immediate and sustained release [18]. During the electrospinning processes, the diameter of fiber, size of pore, and surface morphology of film can all be controlled through the adjustment of four parameters, voltage, polymer concentration, solution flow rate and collector distance [19]. Moreover, a new technique with pressurized gyration and centrifugal spinning was developed for inducing mass production and easier production. The sprayer of pressurized gyration equipment has 20 small dimension roundshaped orifices, with the help of high rotating speed and ~2×pressure, this equipment can realize a large scale and a higher manufacturing throughput [20]. With the help of the increasing spinning speed and pressure, the total process time is much less than normal electrospining [21].

In this work, we fabricate a sandwich structured film matrix for GLP and GLT sustained release by electrospinning of polyvinylacetate (PVA) and ethyl cellulose (EC) which both are biocompatible, no-toxic and biodegradable polymers (Scheme 1). The structure of the sandwiched film consist of an outer layer of GLT (hydrophobic drug) loaded EC fiber, and an inner layer of GLP (hydrophilic drug) loaded PVA fiber. This novel material was expected to provide for the comprehensive utilization of the bioactivities from *G. lucidum*, i.e., the direct cytotoxicity to tumor cells of GLT at first, followed by the proliferation inhibition of GLP. The morphology, structure, biocompatibility, and the release profile of the encapsulated GLP and GLT of this fabricated composite were characterized. The *in vitro* antitumor effects of this composite were studied using human gastric carcinoma cells and human colon cancer cells. And the way of the drug intake was implant. We suggest that a sustained release material with multi-component antitumor drugs should be useful for the comprehensive application of traditional Chinese medicine.

2. Materials and methods

2.1. Materials

GLP and GLT were extracted from *G. lucidum* in our laboratory followed the previous protocol [22,23]. In brief, GLP was a pure polysaccharide purified through DEAE Sepharose Fast Flow ion-exchange chromatography. GLT were consist of Ganoderenic acid D, Ganoderenic acid E and Ganoderenic acid H (1:1:1), prepared from semi-preparative HPLC. PVA (n = approx. 1700) was purchased from Tokyo Chemical Industry (Tokyo, Japan). Ethyl cellulose (EC) (n = approx. 194) was purchased from Shanghai Macklin Biochemical (Shanghai, China). Glucose, vanillin, ursolic acid and perchloric acid were purchased from Aladdin Chemistry (Shanghai, China). Human cervical carcinoma cell lines (Hela cells), human lung cancer cell lines (A549 cells), human gastric carcinoma cell lines (SGC-7901 cells), and human colon cancer cell (Caco-2 cells) were purchased from Institute of Biochemistry and Cell Biology (Shanghai, China). Cell culture medium, PBS (pH = 7.2), Trypsin-EDTA, foetal bovine serum were purchased from Gibco (USA). MTT (3-(4,5)-dimethylthiazol-2-yl)-2,5-diphenyl tetrazolium bromide), dimethylsulfoxide (DMSO), penicillin and streptomycin were from Sigma (St. Louis, USA).

2.2. Preparation of sandwich structured films

2.2.1. Solution configuration

The extraction of crude GLP followed by a water extraction-alcohol precipitation method. Approximately 50 g of *G. lucidum* fruiting body water extraction spray powder was dissolved in 2 L of ultrapure water, and precipitated overnight through adding 8 L ethanol to get polysaccharide. After centrifugation to obtain the precipitation, crude GLP (8000 rpm, 10 min). The pure GLP was purified through DEAE Sepharose Fast Flow ion-exchange chromatography (XK 26 mm × 100 cm, GE, USA), obtained after vacuum freeze-dried (BTO-3XL, Virtis, USA) and stored at 4 °C. Some structural identification of GLP were shown in Fig. S. 3.

The extraction step of GLT was that putting 200 g dry *G. lucidum* fruiting body powder into 5 L 95% alcohol overnight, followed by concentration of the extract and dispersion into ultrapure water, after extracting with petroleum ether extracting and ethyl acetate (EA) (2:1 v/v) in sequence, the EA containing extract were purified through semi-preparative liquid phase (Waters 2535, USA) to get three GLT fractions (Ganoderenic acid D, Ganoderic acid F and Ganoderic acid H), obtained by vacuum freeze-drying and refrigerated at 4 °C. Some structural identification of GLT were showed in Fig. S. 4.

Pure PVA solution (8 w/v%) was prepared by dissolving 8 g PVA powder into 92 mL ultrapure water with magnetic stirring overnight to achieve a homogeneous mixture. GLP freeze-dried powder was added into the PVA solution at a ratio of 12.5%: 1 w/v with magnetic stirring (~300 rpm, 25 °C) to obtain electrospinning solution. And pure EC solution (20 w/v%) was prepared the same way, simply replacing the solvent with ethanol, GLT was added into the EC solution in 60%: 1 w/v under magnetic stirring for subsequent electrospinning.

2.2.2. Electrospinning

Sandwich structure films were fabricated through electrospinning as showed in Schematic 1. The three layers of films were all fabricated using a single needle electrospraying system (TEADFS-103, Xinrui Baina Co., Ltd., China). The system was comprised of stainless steel spinnerets with different gauges (18-gauge needle tip for the EC complex, and 21-gauge needle tip for the PVA complex), precision syringe pumps, metal drum carpeted with tinfoil. The spinneret was connected to the positive electrode, and the metal drum was connected to the negative electrode. The electrospinning order was GLT/EC solution, GLP/PVA solution, and finally GLT/EC solution, the drum diameter is 12 cm, rotation rate is 10 rpm/min.

For the middle layer, approx. 5 mL GLP/PVA solution was suctioned using a syringe for electrospinning. The distance between tinfoil and needle tip was 15 cm, and the flow rate of syringe pump was set at 0.01 mL/min. The electrospinning process was carried out at a voltage of 16 kV, at ambient temperature of ~25 °C and at ~55% relative humidity.

For both of the outer layers, each layer used 5 mL GLT/EC solution, and the other parameters were also modified, e.g., the distance, flow rate, and voltage were 10 cm, 0.008 mL/min, and 21 kV, respectively.

2.3. Characterization

The surface morphology, dimension, and cross fracture of the film were observed through scanning electron microscopy (SEM) (SU8010, Hitachi, Japan). Sample preparation relied on the following steps: films were placed on a metallic sample holder with conductive adhesive tapes, and small pieces of films were treated with liquid nitrogen for the observation of fracture sections. Finally, the surface of films was treated with gold sputtering for ~90 s. The diameters of the fibers obtained were determined from 100 random fibers in each film and calculated using Nano Measurer software.

The compositions of films were analyzed using Fourier transform infrared (FTIR) spectroscopy. The freeze-dried powders of GLP/GLT were detected using KBr die method, i.e., mixing ~3 mg GLP/GLT powders with ~200 mg KBr powder in a jade mortar with grinding, and then placing the mixture into a tablet press machine under 15 MPa and compressing for 3 min. The surfaces of this sandwich film were analyzed using attenuated total reflectance-fourier transform infrared (ATR-FTIR). The transparent sheet or films were scanned by FTIR (Nicolet 6700, Thermo Scientific Nicolet, USA) with a resolution of 4 cm^{-1}, ranging from 4000 to 500 cm^{-1}. Each spectrum was obtained using 32 scans.

X-ray diffraction (XRD) patterns (X'Pert PRO, PNAlytical, Netherlands) were recorded with a powder diffractometer using Cu Kα radiation (λ = 0.1541 nm). The working voltage and current were 40 kV and 40 mA. The patterns were collected with a 2θ range from 5° to 60° at a step of 0.033°, using a X'Celerator detector.

The thermal behaviors of the sample was evaluated through thermogravimetric analysis (TGA, TA-Q800, USA). Around 2–10 mg sample were put into the sealed pans, and heated under a flow of nitrogen gas from 25 to 400 °C (with 10 °C/min rate).

2.4. Hydrophilicity

Before detection, we cut the films into fixed size square (2 × 2 cm) to fabricate the samples. The samples were then fixed on the glass slide using double-sided adhesive tape.

The water contact angle of this sandwich films was measured with a video contact angle instrument (OCA30, Dataphysics, Germany). A water droplet was shed on the surface of the three layers. Photos of the droplet over time were recorded with a high-speed camera. And the contact angles (θ) were obtained using the accompanying software.

The drop infiltration time was also recorded during the wetting process.

2.5. Loading capacity and encapsulation efficiency

The films were cut into small pieces, and dissolved in deionized water or ethanol, respectively, and stirred at room temperature for 5 days. Loading capacity (LC) and encapsulation efficiencies (EE) of GLP and GLT were calculated according to phenol-sulfuric acid method [24], vanillic aldehyde-acetic acid, and perchloric acid method [25]. LC and EE of GLP in PVA film and GLT in EC film were both determined according to eq (1) and eq (2), respectively.

$$LC(\%) = \frac{amount\ of\ GLP\ or\ GLT\ encapsulated\ in\ the\ film\ (mg)}{weight\ of\ the\ film\ (mg)} \times 100\% \quad (1)$$

$$EE(\%) = \frac{amount\ of\ GLP\ or\ GLT\ encapsulated\ in\ the\ film\ (mg)}{theoretical\ total\ amount\ of\ GLP\ or\ GLT\ (mg)} \times 100\% \quad (2)$$

2.6. In vitro release

Drug sustained release was assessed in PBS (pH = 7.2). Sandwich films (14.7 mg) were placed into 10 mL PBS with mild magnetic stirring for 72 h at 37 °C [26]. At specified time interval, 2 mL of the supernatant was removed from the dissolution medium and was replaced with 2 mL fresh PBS. The collected solution was centrifuged to remove indissoluble component (10,000 rpm, 10 min), and GLP/GLT contents were detected using phenol-sulfuric acid method and vanillic aldehyde-acetic acid and perchloric acid method using a 752 N spectrophotometer (Shanghai Jingke, China). The GLP/GLT release curve was drawn based on the quantity of detected drugs over time using eq (3), each sample was measured three-times for error analysis.

$$\text{GLP/GLT release}(\%) = \frac{\text{quantity of GLP/GLT released at time T}}{\text{total quantity released}} \quad (3)$$

2.7. Drug release kinetics

For studying the kinetics and mechanism of the GLP/GLT release, the data for the *in vitro* release tests were fitted to a variety of kinetic equations [27], e.g., zero order (eq (4)), first order (eq (5)), Kopcha model (eq (6)), Makoid-Banakar model (eq (7)), Higuchi's model (eq (8)) and Korsmeyer-Peppas model (eq (9)).

$$M_t = K_0 \cdot t \quad (4)$$

where t is time, M_t is the amount of GLP/GLT releases at time t, respectively, K_0 is the zero order rate constant.

$$M_t = M_\infty \times \left(1 - e^{-K_1 \cdot t}\right) \quad (5)$$

where t is time, M_∞ is the total fraction of GLP/GLT released from the film, and M_t is the amount of GLP/GLT releases at time t, respectively, K_1

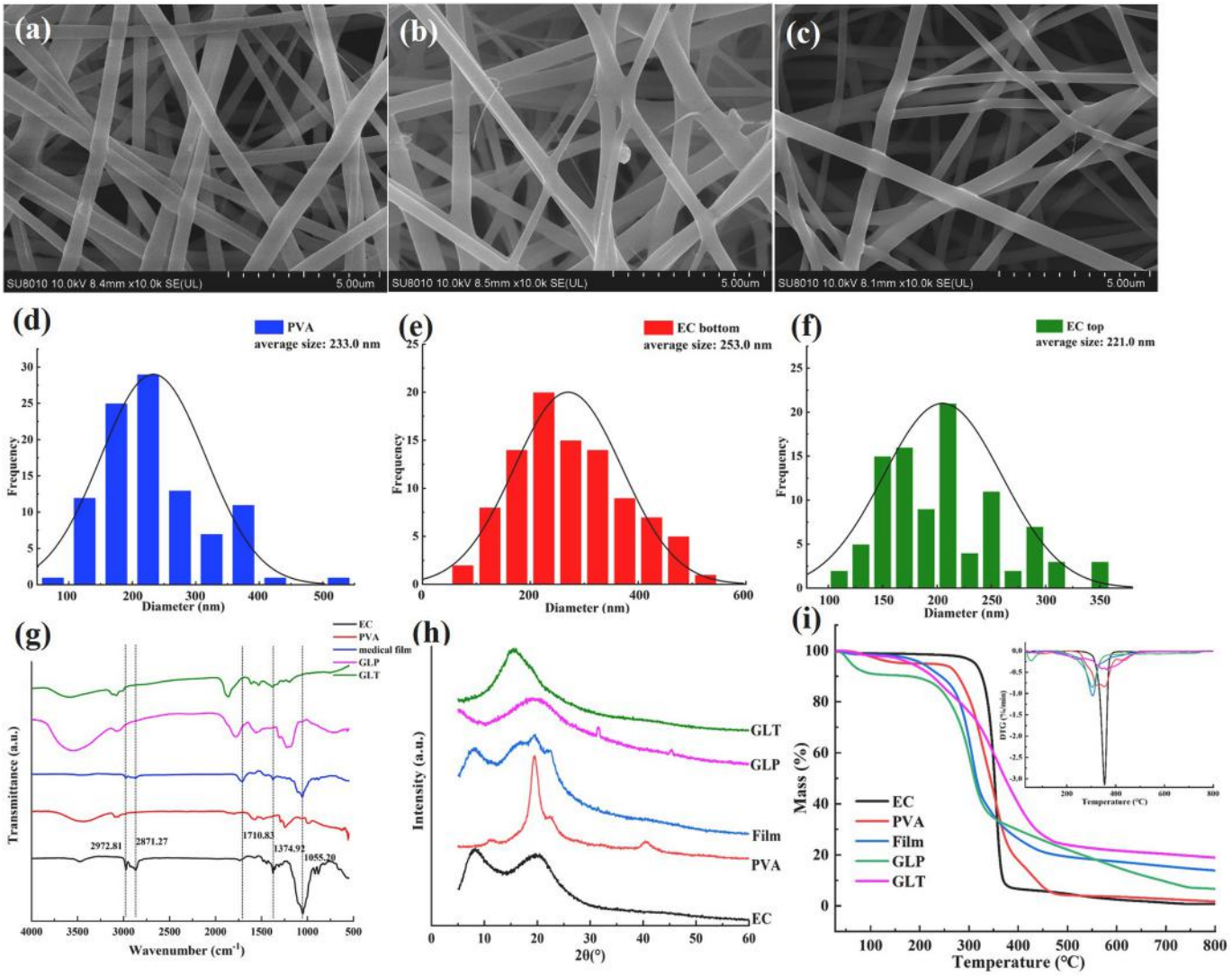

Fig. 1. (a)–(c): SEM results of the middle layer of PVA fiber, the bottom layer of EC fiber, the top layer of EC fiber. (d)–(f): Size distribution of middle layer, bottom layer, and top layer. (g): the FTIR results of EC, PVA, medical film, GLP, and GLT. (h): XRD patterns of EC, PVA, medical film, GLP, and GLT. (i) TGA results of EC, PVA, medical film, GLP, and GLT.

is the first order release constant.

$$M_t = A\cdot\sqrt{t} + B\cdot t \tag{6}$$

where t is time, M_t is the amount of GLP/GLT releases at time t, A and B is Kopcha constant.

$$M_t = K_{MB}\cdot t^n \cdot e^{-ct} \tag{7}$$

where t is time, M_t is the amount of GLP/GLT releases at time t, K_{MB} is Makoid-Banakar coefficient, c is constant, n is the release exponent.

$$M_t = M_0 + K_H\cdot\sqrt{t} \tag{8}$$

where t is time, M_0 and M_t is the amount of GLP/GLT releases at time 0 and t, K_H is the Higuchi dissolution constant.

$$M_t = K_{KP}\cdot t^n \tag{9}$$

where t is time, M_t is the amount of GLP/GLT releases at time t, K_{KP} is Korsmeyer-Peppas constant, n is the Korsmeyer-Peppas release exponent indicating the GLP/GLT release mechanism, when $n < 0.5$ (0.45) represents Pseudo-Fickian diffusion, $n = 0.5$ (0.45) means Diffusion mechanism, $0.5 < n < 1$ (0.89) represents Non-Fickian diffusion (diffusion and erosion), $n = 1$ means Case 2 transport (zero order release), $n > 1$ (0.89) represents Super Case 2 transport (erosion or relaxation).

2.8. Cell culture and in vitro antitumor activity assay

Caco-2 cells were grown in T25 Carrel flask, with total 5 mL cell culture medium, contained Dulbecco's modified eagles medium (DMEM) with low glucose containing L-glutamine, and supplemented with 100 U/ml penicillin, 100 μg/mL streptomycin, and 20% fetal bovine serum (FBS) at 37 °C in a humidified atmosphere of 95% air and 5% CO_2. A549 cells were grown in DMEM contained 10% FBS, Hela and SGC-7901 cells were grown in Roswell Park Memorial Institute (RPMI) 1640 medium contained 10% FBS, these three cell lines were all grown at the same conditions as Caco-2.

For evaluation of the antitumor effects of free GLP, free GLT, and sandwich drug films, 3-(4,5-dimethylthiazo 1-2-yl)-2,5-diphenyltetrazolium bromide (MTT) colorimetric assay was implemented. Cell lines (~1×10^4 cells/well) were seeded in 96-well plates and incubated at 37 °C for 24 h. Then, GLP and GLT freeze-dried powders were dissolved in medium containing a small amount of DMSO (0.1%), passed through a 0.22 μm filter, and drug-loaded films were cut into pieces containing the same drug concentration with the free drug, sterilized by ethylene

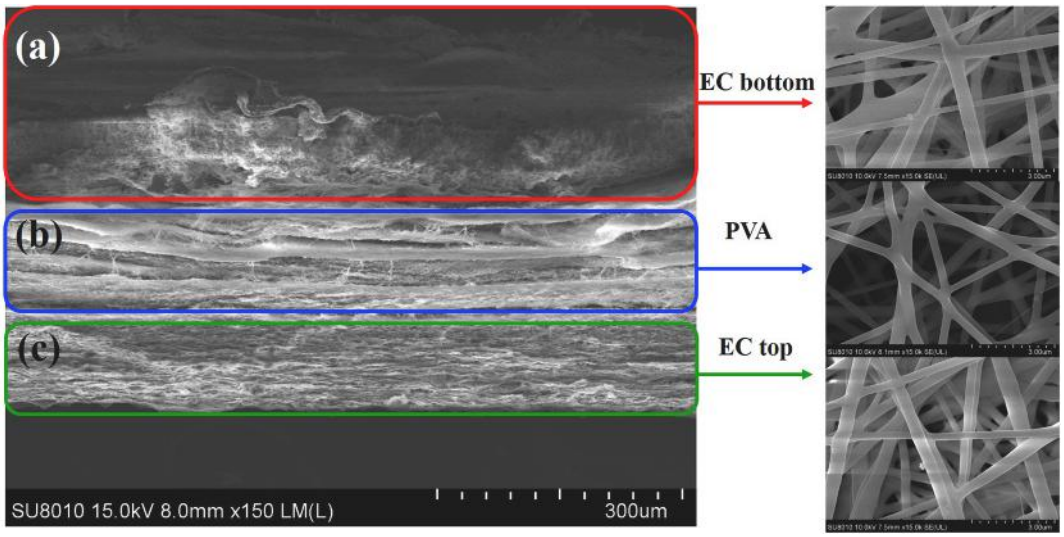

Fig. 2. The cross fracture sections of films.

oxide for 16 h before use. The drug was put into the well of a 96-well plate, incubated for 48 h, after which 20 μL of MTT solution (5 mg/mL) was added into each well, and the plate was incubated for 4 h. At last, removing the supernatant, 100 μL DMSO was added and the absorbance was measured at 570 nm using a micro-plate reader (SpectraMax M5, Molecular Devices, USA).

Cell cycle and apoptosis analyses were measured as described in previous reports [28,29], using cell cycle staining kit and Annexin V-FITC/PI apoptosis kit (MultiSciences, China) by BD Accuri C6 Plus flow cytometer (BD Biosciences, USA) through FlowJo V10 software (BD Biosciences, USA).

Cells were incubated with drug films (10^5 cells in 1 mL) for 24 h in the dishes for observation by confocal laser scanning microscope (CLSM). After which, the culture medium was removed and the cells were washed with PBS (without Ca^{2+} and Mg^{2+}), stained with Hoechst 33342 stain for 10 min, washed 5-times with PBS (without Ca^{2+} and Mg^{2+}), and stained with propidium iodide (PI) stain for 10 min and washed 5-times with PBS (without Ca^{2+} and Mg^{2+}). Finally, the cells were incubated in PBS (without Ca^{2+} and Mg^{2+}) for CLSM observation (Zeiss LSM 880, Germany).

2.9. Statistical analysis

All experiments were performed in triplicate and data is given as mean ± standard deviation (n = 3). One-way analysis of variance (ANOVA) based in LSD method was used to determine the correlation coefficient (R^2) of fitting curve. All statistical plots were plotted using Origin software (OriginLab, USA).

3. Results and discussion

3.1. Film fabrication

The sandwich films were produced using a single electrospining setup, and the process is shown in Schematic 1. The fabricated sandwich films were received on aluminum foil [12]. Schematic 1 also emphasizes the interspersion of GLP in the middle PVA layer or GLT spreads in the outer EC layers. The morphology of this film was light yellow for the existence of GLT, but the inner layer was the primary white color of PVA, because the PVA film and GLP were white. Moreover, the thickness of the film was around 1.50 mm, the thickness of the top layer of EC and inner layer of PVA were both 0.375 mm, and the thickness of the bottom layer of EC was around 0.750 mm.

3.2. Characterizations

SEM results of the middle, bottom, and top layers of the sandwich films are shown in Fig. 1 a, b, and c. The size distribution of middle, bottom, and top layer fibers, at average diameters of 233.0 ± 7.0 nm, 253.0 ± 11.0 nm, and 221.0 ± 3.0 nm are shown in Fig. 1 d, e, and f. The outer layers of EC films are not as uniform as the middle layer. This may be due to the increased viscosity with the volatilization of ethanol during electrospinning [30], and with the addition of GLT powder the volatilization also increased.

The FTIR spectra of several materials are shown in Fig. 1 g. In the top and bottom of the drug film, the EC contained GLT and an O–H stretching band was found at ~3490 cm^{-1} with C–H stretching at ~2972 and ~2871 cm^{-1}, carbonyl stretching from cellulose at ~1710 cm^{-1}, CH deformation vibrations at ~1400 cm^{-1}, and C–O stretching from asymmetric oxygen bridge at ~1055 cm^{-1}. The spectrum of drug film was similar with EC, demonstrating that GLT was loaded within the EC fiber. Both of PVA and GLP had strong O–H stretching band, so they could connect each other through hydrogen bound.

Shown in Fig. 1 h, the physical changes and crystal structures were detected through XRD analysis. All of the GLT, GLP, and EC exist in amorphous form, which are consistent with other researches [31–33]. A peak was shown in $2\theta = 20^\circ$ for PVA. The XRD pattern of the sandwich structure film were same as EC′s, even though loaded drugs. The amorphous form of GLT and GLP could be good for solubility, dissolution rate, and adsorption in the body [32].

Moreover, the thermal behaviour was evaluated through TG analysis. Fig. 1 i shows the TGA thermograms results and DTG curve. Our film is thermally stable up to a temperature of 127.11 °C, the decomposition of it occurs between 127.11 °C and 442.42 °C, and the carbonation reactions begin when the temperature up to 442.42 °C. The decomposition temperature of EC, PVA, GLP, GLT, and film were 317.62 °C, 243.86 °C, 97.21 °C, 184.89 °C, and 207.92 °C, respectively. However, a different TGA profile and DTG curve was captured when drugs are loaded in the film. The degration step of film was lower than pure EC and PVA powder, but higher than GLP and GLT, this may be the result of hydrogen bound between PVA and GLP. The DTG curve of film showed that the rate of mass loss is fastest at 305.32 °C, which are lower than that of EC and PVA. And the peaks of GLT and GLP are not seen in the DTG curve of film, so it is confirmed that the GLT and GLP are exist in the amorphous state in the film fibers [32].

The fracture sections of films, Fig. 2 a-c correspond to the bottom layer of EC containing GLT, the middle layer of PVA containing GLP, and the top layer of EC containing GLT, respectively. The borders of three

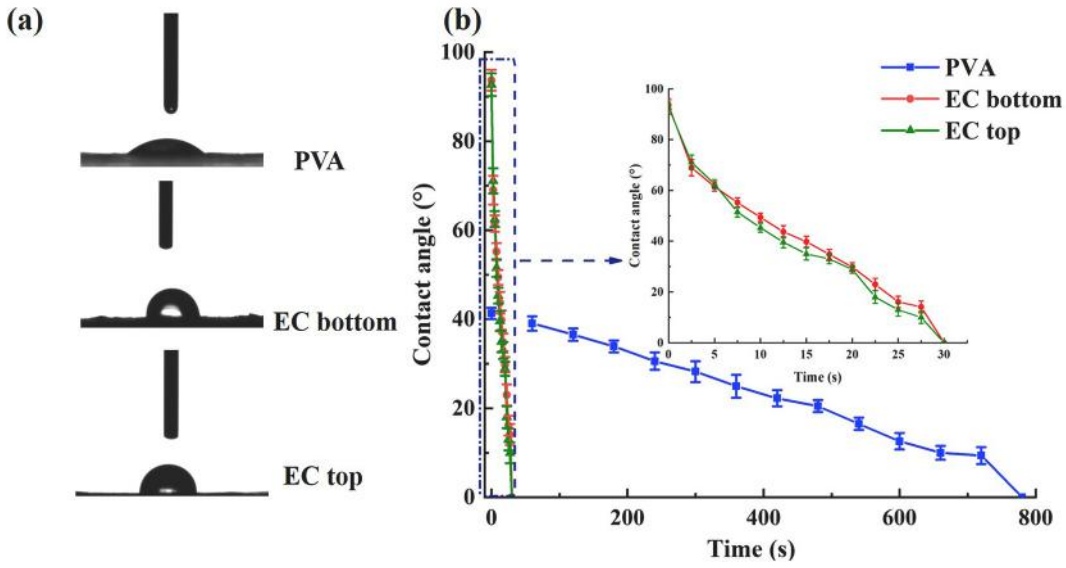

Fig. 3. (a) Water contact angle of the three layers at the beginning of pouring on the surface. (b) Soak times of three layers.

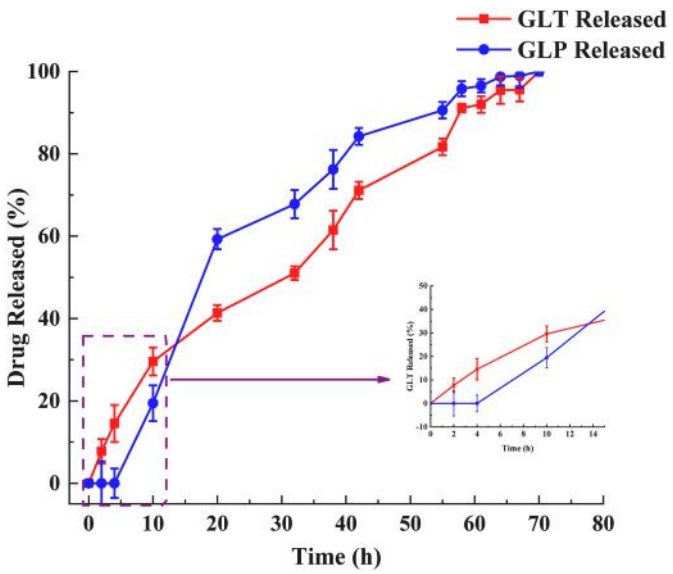

Fig. 4. Cumulative release of GLP/GLT.

layers were obvious.

3.3. Water contact angle

The water contact angle (WCA) of three layers at the beginning of water pouring on the surface are shown in Fig. 3a. The angles were 41.3° (PVA), 93.7° (EC bottom), and 92.7° (EC top). Demonstrating that the middle layer was hydrophilic, the top and bottom layers were hydrophobic. The outer layers were all hydrophobic, but the WCA were different because of the pore diameter differences and surface roughness. The pore diameter of bottom layer was smaller than that of the top layer, and showed more roughness [34] than the top layer.

The decrease of WCA of the three layers is shown in Fig. 3b. The decreased soaking time of the middle layer was much greater than that of the outer layers. One reason for this is the smaller pore diameter of the middle layer and another reason is that the –OH groups were embedded at first, the number of hydrophilic groups will expose to water later [35, 36].

It is reported that when the rate of water penetration into the matrix decreases, the drug release would be sustained [37]. So our antitumor process could be that GLT in the outer layers is first released to kill the tumor cells after which GLP in the middle layer is released to further inhibit the proliferation of tumor cells. Furthermore, the sustained release GLP and GLT can then continually exhibit an effect on the tumor cells.

3.4. GLP and GLT content

The loading capacity (LC) of GLT and GLP were 1.6% ± 0.3% and 7.9% ± 0.2%, the encapsulation efficiencies (EE) of GLT and GLP were 83.80% ± 0.07% and 20.62% ± 0.04%.

3.5. In vitro drug release and kinetics

The *in vitro* data obtained from GLP and GLT release studies from all loaded fibers were plotted as a cumulative percent of drug released *vs* time and is shown in Fig. 4. Both EC layers and PVA layer have similar drug release profiles. In the first 4 h, only GLT showed burst release, because the three layers did not separate, then GLP showed burst release within 20 h. After 20 h, both of GLT and GLP showed sustained release until 70 h. The burst release is because of the large surface area and the releasing of the GLP/GLT in the surface of the fibers, and the sustained release is because of the dissolution process of the PVA [38], and the diffusion of GLT. Moreover, the release profile is also effected by the fiber morphology [39], the fiber with smaller diameter and the more rough surface both contribute to the release rate. In theory, a higher drug loading contribute to a longer release time, but the release time were almost same of GLP (7.9% LC) and GLT (1.6% LC), it might be also effected by the hydrophilic-hydrophobic property of drugs.

After stirring for about 4 h, the EC layers were broken into pieces, and the PVA layer were exposed to the solution. Due to the insolubility of EC in water, the GLT release step resulted from diffusion out of the fiber to the solution.

PVA is water-soluble, thus, the breakdown of EC layers and the exposure of PVA layer results in an initial burst release began from out of the fiber. The slow release of GLP is due to hydrogen bonding between the –OH groups of GLP and PVA, and GLP release from the inner fiber, this could be verified by the xanthan gum (XG) (an anionic polysaccharide) bonding with PVA through the hydrogen bond [40].

In this work, various kinetic equations were fitted to the

Table 1
The IC_{50} of GLT/GLP solution and medical films to several human tumor cells (n = 5).

Cell name	IC_{50} of medical solutions (μg/mL)	IC_{50} of medical films (mg)/the concentration after conversion (μg/mL)
SGC-7901	93.8 ± 4.3	0.66 ± 0.05/51.2 ± 3.9 *
A549	107.8 ± 1.1	1.17 ± 0.21/90.7 ± 16.3
Hela	128.1 ± 2.2	1.20 ± 0.34/93.0 ± 26.4
Caco-2	98.8 ± 1.6	0.28 ± 0.08/21.7 ± 6.2 **

Possibilities less than 0.05 was considered significant and significant levels were expressed as $*p < 0.05$, $**p < 0.01$

experimental GLP/GLT release data, with the best kinetic model being obtained by evaluating the regression coefficient. The drug release mechanisms were revealed using various kinetic models. And the data of the matched model were showed in Table S. 1.

The release profiles were not linear so GLP release and GLT release were not zero- order (Fig. 4). The release of GLP/GLT occurred in two stages: first, an initial burst release stage, followed by a slow release stage associated with diffusion. The fitting results revealed that GLP/GLT release in PBS were both best fitted with Kopcha model, since, R^2 of Kopcha model (0.982 and 0.976) were a little more than Korsmeyer-Peppas model (0.981 and 0.976). Moreover, the *A* (diffusion term)/*B* (erosion term) ratio, obtained from the Kopcha model, also indicated the release mechanism, i.e., when the ratio was far greater than 1, the release mechanism was mainly by Fickian diffusion [41]. According to this theory both of the GLP and GLT release mechanisms are in accordance with Fickian diffusion.

3.6. Tumor cells inhibition assay

3.6.1. Cell proliferation inhibition

Tumor cells were treated with different concentrations of tested drugs for 24 h and then tested using MTT assay. Free PVA and EC films displayed almost no cytotoxicity against tumor cells, however, the drug films all showed better tumor inhibitory effects than the drug solutions, which contained almost same GLP and GLT doses as drug films (Fig. S. 1). This may be the result of sustained release, prompting the duration of the effective concentration [42]. The IC_{50} of GLT/GLP solution and this drug-containing film were calculated using SPSS software (IBM, USA), the results are shown in Table 1.

3.6.2. Cell cycle and apoptosis

Both Hela and Caco-2 cells cycles were arrested in G1 phase after treatment, but A549 and SGC-7901 were arrested in G2 phase (Fig. 5). Cell apoptosis rates were 62.9% ± 1.3%, 61.9% ± 2.1%, 94.1% ± 2.2%, 65.3% ± 1.8% (Hela, A549, SGC-7901, Caco-2), respectively (Fig. 6). This drug could promote all of the cells to enter the apoptosis stage, but the apoptosis ratio also existed differences between tumor cell lines, and our drug had a better therapeutic effect on the gastric cancer. The therapeutic efficiency was also confirmed by CLSM (Fig. 7), i.e., the red fluorescence is attributed to apoptotic cells, while the blue fluorescence represents the living cells. Because hoechst 33342 stain belongs to non-embedded fluorescent dyes, it is connect with the trenches in the enrichment region of A and T nucleobase sequence of living cell, presenting blue fluorescence; PI stain could embed in the DNA of apoptosis and necrotic cell, presenting red fluorescence. So we concluded that our antitumor medical film could induce the apoptosis of several human tumor cell lines. The results of fluorescence staining also demonstrate the good efficiency of this medicine films *in vitro* treatment.

4. Conclusions

Specific antitumor drug delivery films, based on the sandwich structure with high drug loading capacity and good encapsulation efficiency, were fabricated using electrospinning. Both top and bottom layers consist of a hydrophobic polymer containing non-water-soluble GLT with a hydrophilic layer containing water-soluble GLP in between the outer layers. The borders among layers are clear and the layers gradually separate and break into pieces for further drug release when dissolving in water. This specific antitumor film delivers the bioactivities of both GLP and GLT, i.e., demonstrating the activities of inhibiting tumor cell invasion, restricting the proliferation and inducing

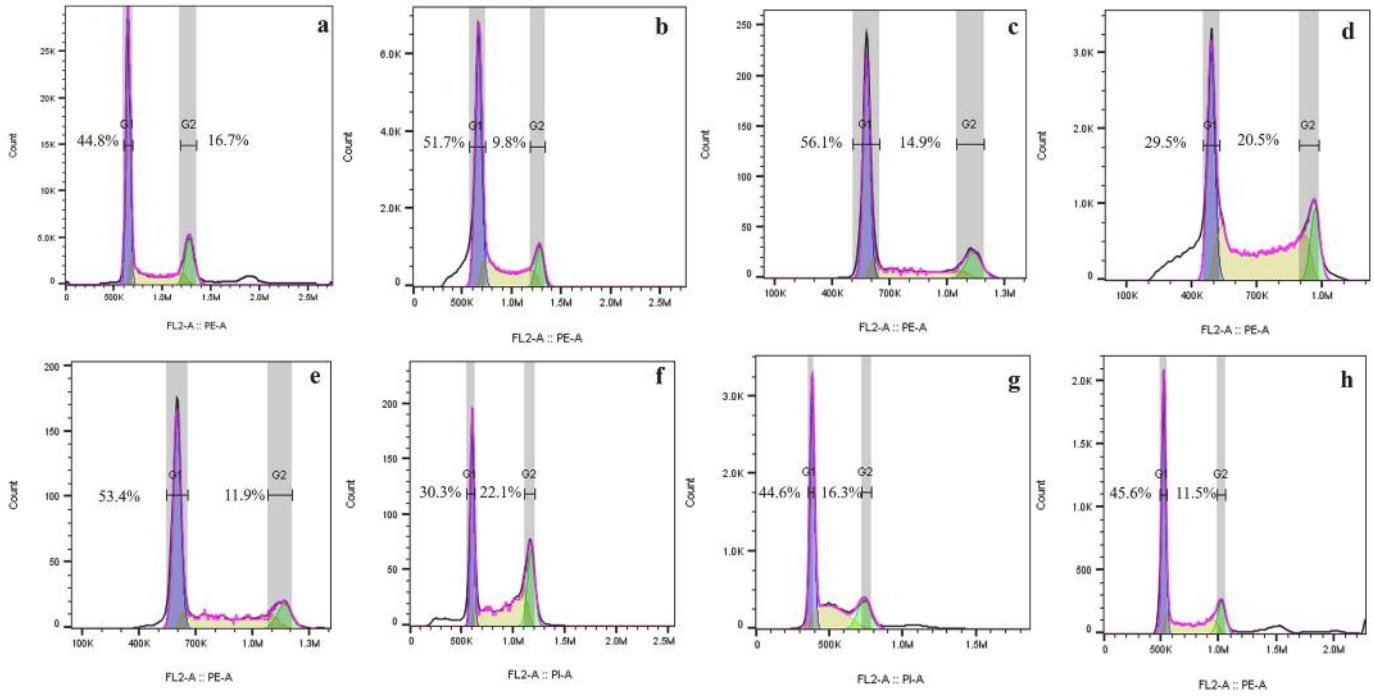

Fig. 5. Cell cycle of Hela, A549, SGC-7901 and Caco-2 cells. a) normal group of Hela cell; b) medicine group of Hela cell; c) normal group of A549 cell; d) medicine group of A549 cell; e) normal group of SGC-7901 cell; f) medicine group of SGC-7901 cell; g) normal group of Caco-2 cell; h) medicine group of Caco-2 cell.

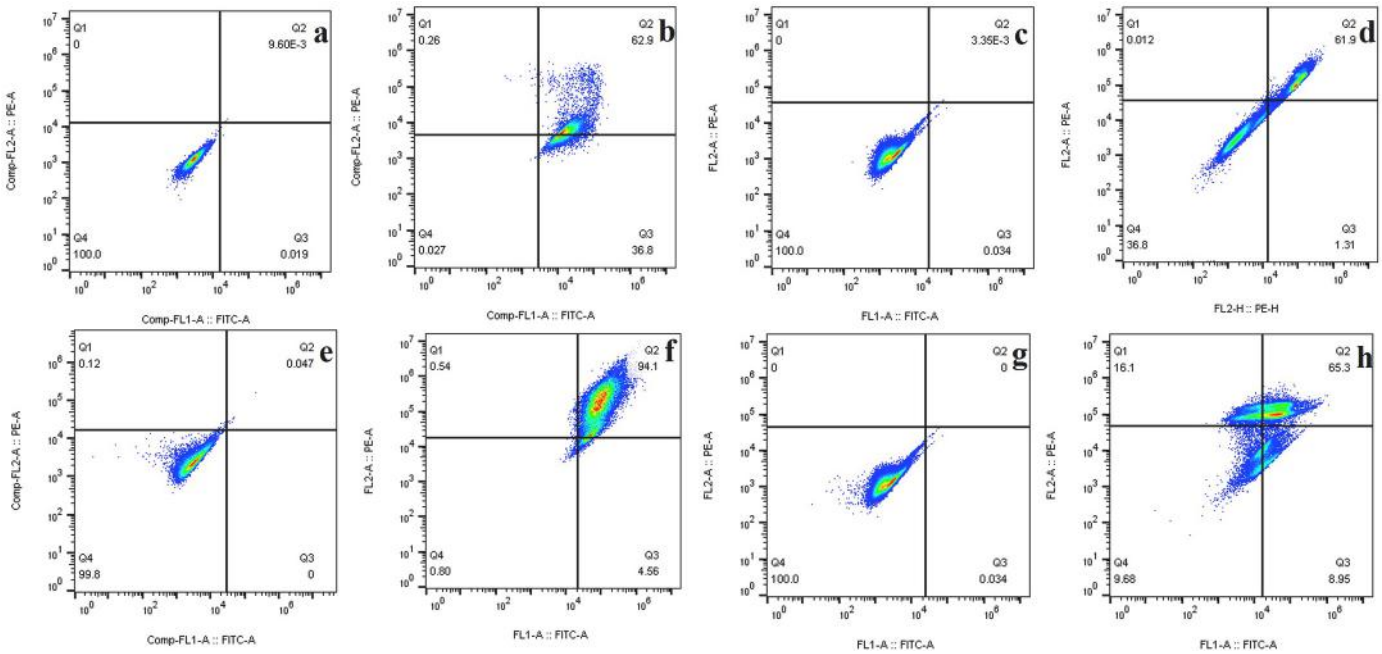

Fig. 6. Cell apoptosis of Hela, A549, SGC-7901 and Caco-2 cells. a) normal group of Hela cell; b) medicine film group of Hela cell, the apoptotic rate was 62.9%; c) normal group of A549 cell; d) medicine film group of A549 cell, the apoptotic rate was 61.9%; e) normal group of SGC-7901 cell; f) medicine film group of SGC-7901 cell, the apoptotic rate was 94.1%; g) normal group of Caco-2 cell; h) medicine film group of Caco-2 cell, the apoptotic rate was 65.3%.

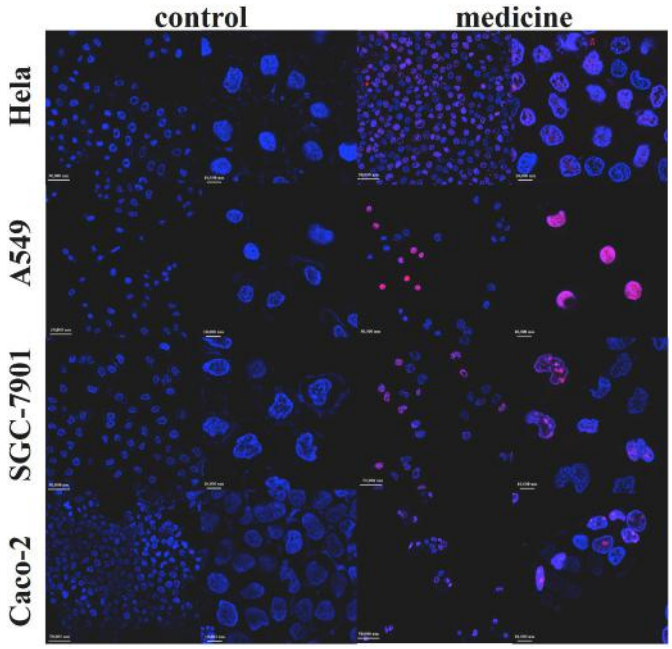

Fig. 7. CLSM observation of cells after hoechst 33342 and PI stain. Scale bars represent 10 μm and 50 μm.

apoptosis of tumor cells, tumor cell cycle arrest modulation, and direct cytotoxicity. Importantly, the effects of a multicompounded drug and sustained release effectively inhibit tumor cells. Compared with the inhibition effects to Hela and A549 cell lines of GLP-loaded chitosan nanoparticles, the IC_{50} of our drug were much lower, and this antitumor drug formulation do not possess the ability of sustained release [43]. Another research is about encapsulating GLP in flexible PVP membrane through electrospining, and unfortunately, the release of GLP was just a burst release [44]. So far, there is a research article about the GLT sustained release, it was about ganoderic acid loaded in solid lipid nanoparticles, but its time of controlled release was only 24 h, the entrapment efficiency (70.16%) was lower than ours, and the usage of it was not in the antitumor field [45]. Moreover, another research was about the fabrication of a drug loaded core-shell fibrous system, used for cervical cancer therapy [32]. GLT was loaded in polycaprolactone as the core layer. That structure with GLT embedded in the core layer, can greatly decrease the oxidation of GLT. The release of GLT was much longer (168 h) than ours (70 h), it is may because GLT was loaded in the outer layers in our structure. And the carrier material was also different. The *in vitro* anti-cancer effects were similar, but cell cycle arrest and cell apoptosis for four tumor cells were further explored by us. Finally, our specific antitumor drug showed promising properties for the effective enhancement. For the further study on *G. lucidum*, the relationship between intestinal flora and antitumor activity of GLP can be exploited. Moreover, the rheological property of GLP may have some effects on the characters of electrospining fibers. For example, the fiber linear density and unseparated fiber percentage both showed an increasing trend as the increasement of polysaccharides [46].

CRediT authorship contribution statement

Jiahui Lu: Data curation, Writing – original draft, preparation, Visualization. **Yanying Li:** Investigation. **Anqiang Zhang:** Term, Supervision, Writing – review & editing, Reviewing and Editing. **Weiming Liu:** Funding acquisition. **Xingli Wang:** Funding acquisition. **Fuming Zhang:** Validation, Writing – review & editing, Reviewing and Editing. **Robert J. Linhardt:** Validation, Writing – review & editing, Reviewing and Editing. **Zhibin Lin:** Writing – review & editing, Reviewing and Editing. **Peilong Sun:** Resources, Project administration, Supervision.

Declaration of ompeting interest

The authors declare that they have no known competing financial interests or personal relationships that could have appeared to influence the work reported in this paper.

Acknowledgments

This project is supported by the fund from National Key Research and Development Project of China (Grant No. 2018YFC2001803) and Natural Science Foundation of Zhejiang Province, China (Grant No.) LY17C200017.

References

[1] D. Han, A.J. Steckl, Triaxial electrospun nanofiber membranes for controlled dual release of functional molecules, ACS Appl. Mater. Interfaces 5 (16) (2013) 8241–8245.
[2] C.-H. Lee, S.-H. Cheng, I.-P. Huang, J.S. Souris, C.-S. Yang, C.-Y. Mou, L.-W. Lo, Intracellular pH-responsive mesoporous silica nanoparticles for the controlled release of anticancer chemotherapeutics, Angew. Chem. Int. Ed. 49 (44) (2010) 8214–8219.
[3] D. Carson, Y.H. Jiang, K.A. Woodrow, Tunable release of multiclass anti-HIV drugs that are water-soluble and loaded at high drug content in polyester blended electrospun fibers, Pharm. Res. 33 (1) (2016) 125–136.
[4] X. Gong, G. Dang, J. Guo, Y.F. Liu, Y. Gong, A sodium alginate/feather keratin composite fiber with skin-core structure as the carrier for sustained drug release, Int. J. Biol. Macromol. 155 (2020) 386–392.
[5] L. Ma, G. Yang, N. Wang, P. Zhang, F. Guo, J. Meng, F. Zhang, Z. Hu, S. Wang, Y. Zhao, Trap effect of three-dimensional fibers network for high efficient cancer-cell capture, Adv. Healthc. Mater. 4 (6) (2015) 838–843.
[6] J. Zhang, X. Wang, T. Liu, S. Liu, X. Jing, Antitumor activity of electrospun polylactide nanofibers loaded with 5-fluorouracil and oxaliplatin against colorectal cancer, Drug Deliv. 23 (3) (2016) 794–800.
[7] M.R. El-Aassar, E.A. Saad, S.A. Habib, H.M. Waly, Loading of some quinoxaline derivatives in poly (l-lactic) acid/Pluronic F-127 nanofibers enhances their anticancer efficiency and induces a p53 and p21 apoptotic-signaling pathway, Colloids Surf., B 183 (2019) 110444.
[8] J.W.M. Yuen, M.D.I. Gohel, Anticancer effects of *Ganoderma lucidum*: a review of scientific evidence, Nutr. Canc. 53 (1) (2005) 11–17.
[9] D. Sohretoglu, S. Huang, *Ganoderma lucidum* polysaccharides as an anti-cancer agent, Anti Canc. Agents Med. Chem. 18 (5) (2018) 667–674.
[10] L.M.H. Trajkovic, S.A. Mijatovic, D.D. Maksimovic-Ivanic, I.D. Stojanovic, M. B. Momcilovic, S.J. Tufegdzic, V.M. Maksimovic, Z.S. Marjanovic, S.D. Stosic-Grujicic, Anticancer properties of *Ganoderma lucidum* methanol extracts *in vitro* and *in vivo*, Nutr. Canc. 61 (5) (2009) 696–707.
[11] Z. Xing, C. Zhang, C. Zhao, Z. Ahmad, J. Li, M. Chang, Targeting oxidative stress using tri-needle electrospray engineered *Ganoderma lucidum* polysaccharide-loaded porous yolk-shell particles, Eur. J. Pharmaceut. Sci. 125 (2018) 64–73.
[12] L. Zhu, X. Chen, Z. Ahmad, J. Li, M. Chang, Engineering of *Ganoderma lucidum* polysaccharide loaded polyvinyl alcohol nanofibers for biopharmaceutical delivery, J. Drug Deliv. Sci. Technol. 50 (2019) 208–216.
[13] F.F.Y. Radwan, J.M. Perez, A. Haque, Apoptotic and immune restoration effects of ganoderic acids define a new prospective for complementary treatment of cancer, J. Clin. Cell. Immunol. S3 (2011) 4.
[14] P. Li, L. Liu, S. Huang, Y. Zhang, J. Xu, Z. Zhang, Anti-cancer effects of a neutral triterpene fraction from Ganoderma lucidum and its active constituents on SW620 human colorectal cancer cells, Anti Canc. Agents Med. Chem. 20 (2) (2020) 237–244.
[15] E.R. Kenawy, G.L. Bowlin, K. Mansfield, J. Layman, D.G. Simpson, E.H. Sanders, G. E. Wnek, Release of tetracycline hydrochloride from electrospun poly (ethylene-co-vinylacetate), poly (lactic acid), and a blend, J. Contr. Release 81 (1–2) (2002) 57–64.
[16] E.J. Torres-Martinez, J.M.C. Bravo, A.S. Medina, G.L.P. Gonzalez, L.J.V. Gomez, A summary of electrospun nanofibers as drug delivery system: drugs loaded and biopolymers used as matrices, Curr. Drug Deliv. 15 (10) (2018) 1360–1374.
[17] P. Wang, Y. Li, C. Zhang, F. Feng, H. Zhang, Sequential electrospinning of multilayer ethylcellulose/gelatin/ethylcellulose nanofibrous film for sustained release of curcumin, Food Chem. 308 (2020) 125599.
[18] A. Balogh, B. Farkas, A. Palvolgyi, A. Domokos, B. Demuth, G. Marosi, Z.K. Nagy, Novel alternating current electrospinning of Hydroxypropylmethylcellulose Acetate Succinate (HPMCAS) nanofibers for dissolution enhancement: the importance of solution conductivity, J. Pharmaceut. Sci. 106 (6) (2017) 1634–1643.
[19] S.-Y. Ryu, S.-Y. Kwak, Role of electrical conductivity of spinning solution on enhancement of electrospinnability of polyamide 6,6 nanofibers, J. Nanosci. Nanotechnol. 13 (6) (2013) 4193–4202.
[20] S. Mahalingam, R. Matharu, S. Homer-Vanniasinkam, M. Edirisinghe, Current methodologies and approaches for the formation of core-sheath polymer fibers for biomedical applications, Appl. Phys. Rev. 7 (4) (2020), 041302.
[21] H. Alenezi, M.E. Cam, M. Edirisinghe, Experimental and theoretical investigation of the fluid behavior during polymeric fiber formation with and without pressure, Appl. Phys. Rev. 6 (4) (2019).
[22] L. Cao, J. Zhou, F. Zheng, J. Yao, T. Wang, Study on extraction of polysaccharides from *Ganoderma lucidum* by hot compressed water and its antioxidant activities, J. Food Sci. Technol. 36 (2) (2018) 58–62.
[23] W.M. Ruan, A.H.H. Lim, L.G. Huang, D.G. Popovich, Extraction optimisation and isolation of triterpenoids from *Ganoderma lucidum* and their effect on human carcinoma cell growth, Nat. Prod. Res. 28 (24) (2014) 2264–2272.
[24] K.A.C.C. Taylor, A modification of the phenol/sulfuric acid assay for total carbohydrates giving more comparable absorbances, Appl. Biochem. Biotechnol. 53 (3) (1995) 207–214.
[25] D. Qu, J. He, C. Liu, J. Zhou, Y. Chen, Triterpene-loaded microemulsion using coix lacryma-jobi seed extract as oil phase for enhanced antitumor efficacy: preparation and in vivo evaluation, Int. J. Nanomed. 9 (1) (2014) 109–119.
[26] M. Takahashi, H. Onishi, Y. Machida, Development of implant tablet for a week-long sustained release, J. Contr. Release 100 (1) (2004) 63–74.
[27] M. Eltayeb, E. Stride, M. Edirisinghe, A. Harker, Electrosprayed nanoparticle delivery system for controlled release, Mater. Sci. Eng. C 66 (2016) 138–146.
[28] L.L.-Y. Chan, N. Lai, E. Wang, T. Smith, X. Yang, B. Lin, A rapid detection method for apoptosis and necrosis measurement using the cellometer imaging cytometry, Apoptosis 16 (12) (2011) 1295–1303.
[29] W.M. Ruan, Y. Wei, D.G. Popovich, Distinct responses of cytotoxic *Ganoderma lucidum* triterpenoids in human carcinoma cells, Phytother Res. 29 (11) (2015) 1744–1752.
[30] X. Wu, L. Wang, H. Yu, Y. Huang, Effect of solvent on morphology of electrospinning ethyl cellulose fibers, J. Appl. Polym. Sci. 97 (3) (2005) 1292–1297.
[31] L. Huang, D. Yu, C. Branford-White, L. Zhu, Sustained release of ethyl cellulose micro-particulate drug delivery systems prepared using electrospraying, J. Mater. Sci. 47 (3) (2012) 1372–1377.
[32] S. Shen, L. Zhu, J. Liu, A. Ali, A. Zaman, Z. Ahmad, X. Chen, M. Chang, Novel core-shell fiber delivery system for synergistic treatment of cervical cancer, J. Drug Deliv. Sci. Technol. 59 (2020) 101865.
[33] F. Wu, H. Huang, Surface morphology and protective effect of Hericium erinaceus polysaccharide on cyclophosphamide-induced immunosuppression in mice, Carbohydr. Polym. 251 (2021) 116930.
[34] Y. Liu, W. Ning, Q. Wei, Y. Cai, A. Wei, Wetting behavior of electrospun poly(L-lactic acid)/poly(vinyl alcohol) composite nonwovens, J. Appl. Polym. Sci. 110 (5) (2010) 3172–3177.
[35] J. Zhang, W. Zhang, J. Lu, C. Zhu, W. Lin, J. Feng, Aqueous epoxy-based superhydrophobic coatings: fabrication and stability in water, Prog. Org. Coating 121 (2018) 201–208.
[36] G.W. Li, W. Zhang, J.P. Yang, X.P. Wang, Time-dependence of pervaporation performance for the separation of ethanol/water mixtures through poly(vinyl alcohol) membrane, J. Colloid Interface Sci. 306 (2) (2007) 337–344.
[37] K.K. Peh, C.F. Wong, K.H. Yuen, Possible mechanism for drug retardation from glyceryl monostearate matrix system, Drug Dev. Ind. Pharm. 26 (4) (2000) 447–450.
[38] D. Yu, X. Li, X. Wang, J. Yang, S.W.A. Bligh, G.R. Williams, Nanofibers fabricated using triaxial electrospinning as zero order drug delivery systems, ACS Appl. Mater. Interfaces 7 (33) (2015) 18891–18897.
[39] J. Ahmed, R.K. Matharu, T. Shams, U.E. Illangakoon, M. Edirisinghe, A comparison of electric-field-driven and pressure-driven fiber generation methods for drug delivery, Macromol. Mater. Eng. 303 (5) (2018) 1700577.
[40] C.-E. Brunchi, M. Bercea, S. Morariu, M. Avadanei, Investigations on the interactions between xanthan gum and poly(vinyl alcohol) in solid state and aqueous solutions, Eur. Polym. J. 84 (2016) 161–172.
[41] M. Zandi, Evaluation of the kinetics of ascorbic acid (AA) release from alginate-whey protein concentrates (AL-WPC) microspheres at the simulated gastro-intestinal condition, J. Food Process. Eng. 40 (1) (2017) e12334.
[42] X. Hu, R. Han, L. Quan, C. Liu, Y. Liao, Stabilization and sustained release of zeylenone, a soft cytotoxic drug, within polymeric micelles for local antitumor drug delivery, Int. J. Pharm. 450 (1–2) (2013) 331–337.
[43] N. Li, Y. Hu, C. He, C. Hu, J. Zhou, G. Tang, J. Gao, Preparation, characterisation and anti-tumour activity of *Ganoderma lucidum* polysaccharide nanoparticles, J. Pharm. Pharmacol. 62 (1) (2010) 139–144.
[44] S.T. Wu, J.S. Li, J. Mai, M.W. Chang, Three-dimensional electrohydrodynamic printing and spinning of flexible composite structures for oral multidrug forms, ACS Appl. Mater. Interfaces 10 (29) (2018) 24876–24885.
[45] H. Shafique, A. Ahad, W. Khan, M.Y. Want, P.C. Bhatt, S. Ahmad, B.P. Panda, M. Mujeeb, Ganoderic acid -loaded solid lipid nanoparticles ameliorate D-galactosamine induced hepatotoxicity in Wistar rats, J. Drug Deliv. Sci. Technol. 50 (2019) 48–56.
[46] Z. Li, Z. Li, R. Ding, C. Yu, Composition of ramie hemicelluloses and effect of polysaccharides on fiber properties, Text, Res. J. 86 (5) (2016) 451–460.